International Journal of Environmental Sciences
ISSN: 2229-7359
Vol. 11 No. 5s,2025
https://theaspd.com/index.ph

Parametric Optimization And Comparative Study Of Ductile Cast Iron (DCI) 500/7 Grade Material By Using Shielded Metal Arc Welding (SMAW)

Aamir R. Sayed[1], Devesh Kumar[2]
[1*]Research Scholar, Poornima University, Jaipur; arsjdcoe@gmail.com[1]
[1]Faculty of Engineering & Technology, Poornima University, Jaipur; deveshmech19@gmail.com1

Abstract:
Welding is a vital manufacturing technique used to join two or more materials–primarily metals or thermoplastics–by applying heat, pressure, or a combination of both. In this study, the Shielded Metal Arc Welding (SMAW) process was employed to perform parametric optimization on ductile cast iron (DCI) grade 500/7. A total of 18 welded plates were fabricated using two different electrodes, following the L9 orthogonal array (OA) design. These samples were evaluated through both (Destructive Testing) DT–including hardness, impact, and tensile tests–and (Non-Destructive Testing) (NDT) methods such as (Dye Penetrant Testing) DPT, (Magnetic Particle Testing) MPT, (Radiographic Testing) RT, and visual inspection. The study focused on three key input parameters: welding current (100, 110, and 120 Ampere), preheat temperature (250°C, 300°C, and 350°C), and interpass temperature (100°C, 200°C, and 300°C). Corresponding output responses measured included hardness (BHN), impact strength (J), and tensile strength (MPa). A multi-objective optimization was performed using the Taguchi method combined with Grey Relational Analysis (GRA). Results indicated that the B-540 electrode outperformed B-850, delivering superior mechanical properties under the tested conditions. The electrode A-540 shows the more stability and better result as compared to B-850 electrodes. The Interpass temperature shows the dominant parameter for A-540 electrode whereas the Pre heat temperature plays an influential parameter for the electrode B-850. The experiment number 7 gives the best result for the A-540 electrodes satting the current at 120 ampere, preheat temperature at 250°C and Interpass temperature at 300°C. The experiment number 2 states the input parameters as current at 100 ampere, preheat at 300 °C and Interpass temperature at 200 °C for the electrode B - 850.

Keywords: *Welding, SMAW, Orthogonal Array, Taguchi GRA, Destructive testing and Non Destructive Testing.*

INTRODUCTION

Welding is a process used to join materials by melting and fusing them together. Various techniques, such as SMAW, GMAW, GTAW, and FCAW, are utilized in different applications. It plays a vital role in industries like construction and manufacturing, ensuring strong and reliable material bonds. SMAW, commonly referred to as stick welding, is widely employed for metal joining. In this method, an electrode with a flux coating creates an electric arc, melting the electrode and the base material while the flux offers protection and aids in cooling. Ductile Cast Iron (DCI) is well-known for its high strength, toughness, and flexibility. Its ability to deform without breaking makes it ideal for applications such as automotive components, including engine blocks and suspension systems. Additionally, it is widely used in machinery, construction, and agriculture due to its resistance to wear and ease of machining. DCI pipes are particularly prominent in water distribution and sewage systems because of their excellent corrosion resistance and durability. Optimization techniques are strategies designed to identify the best possible solution from a range of viable options. These methods aim to either maximize or minimize specific objectives while adhering to given constraints. Two weld joints of Inconel 617 alloy, fabricated using GTAW and SMAW techniques, demonstrated segregation of Mo and Cr, resulting in the formation of secondary phases. Microstructural examination indicated significant dilution at the interface due to the close melting points of the materials. Mechanical testing, including tensile tests at ambient and elevated temperatures and Charpy impact tests, revealed that the GTAW-welded joints exhibited better mechanical performance, making them more appropriate for service applications [1]. This research examines the influence of shielded metal arc welding (SMAW) parameters on the mechanical properties and angular distortion of SA 516 grade 70 welded joints. The study employs the Taguchi method and Grey relational analysis to optimize factors such as root gap, groove angle, electrode diameter, and preheating temperature. A total of nine experiments were carried out, resulting in enhanced outcomes. Validation through confirmatory experiments affirmed the optimized results, which are vital for manufacturing storage tanks, boilers, and pressure vessels [2]. This study evaluates the effects of root pass removal methods, specifically back grinding and back gouging, on SMAW-welded ASTM A516 grade 70 mild steel joints. Microstructural analysis reveals that back-gouged joints exhibit coarser grains, influencing their mechanical properties. Tensile testing indicates that back-ground joints demonstrate better performance, highlighting the critical role of welding parameters in achieving optimal results [3]. This study investigates the tensile strength of SMAW-welded dissimilar joints of mild steel (MS)

and medium carbon steel (CS). By varying welding current, electrode angle, and root face, the Taguchi L9 orthogonal array is used to determine the optimal parameters for maximum tensile strength. Findings reveal that electrode angle is the most significant factor, contributing 73.97%, followed by root face at 6.24% and welding current at 5.12% [4]. This study focuses on optimizing bead geometry, including reinforcement height, bead width, and left and right leg lengths, by examining the interaction of process parameters. Using the Taguchi L9 orthogonal array, experiments were conducted on 200x400x12mm and 20mm thick S400 plates with CO2 shielding gas, varying welding current (240–280 A), voltage (23–27 V), and speed (40–50 cm/min). A mathematical model and algorithm were developed to control the output parameters, highlighting a direct relationship between increased welding current and enhanced bead geometry[5]. Pulsed Gas Metal Arc Welding (P-GMAW) improves quality and efficiency in advanced manufacturing processes. This study examines the effects of welding parameters on strength and hardness using Taguchi's L27 orthogonal array and the GMDH algorithm. The findings highlight the superior predictive accuracy of the GMDH algorithm compared to multiple regression analysis (MRA)[6]. An experimental study on TIG-welded 304 stainless steel utilized artificial intelligence techniques to analyze performance. Welding parameters, including welding current (WC), welding speed (WS), gas flow rate (GFR), and voltage, were varied to evaluate tensile strength (TS) in MPa. Response Surface Methodology (RSM) was applied with 27 experimental runs using Design of Experiments (DoE), while MATLAB-based ANFIS was used for modeling. The highest tensile strength recorded was 664 MPa under optimal conditions: 50 A welding current, 12 lpm gas flow rate, 1 mm/s welding speed, and 12 V voltage, achieving zero prediction error [7]. The study investigated the microstructural and mechanical properties of Inconel 718 TIG weldments, which are crucial for the aeronautical and aerospace industries. A post-weld heat treatment at 750°C for 8 hours, followed by cooling at 650°C for another 8 hours, was found to optimize these properties. Experiments conducted on 2mm thick specimens identified the optimal welding current range as 60–70A for achieving the best results [8]. Weld quality is influenced by mechanical properties, process variables, and input parameters. This research focuses on optimizing SMAW parameters for ASTM A572 Grade 50 steel joints using the Taguchi L16 orthogonal array. The findings reveal that the groove angle significantly affects tensile strength, electrode diameter impacts impact strength, and welding current influences hardness and distortion, resulting in notable improvements in weld performance [9]. A dissimilar joint of Inconel 718 and 304L stainless steel was welded using gas tungsten arc welding (GTAW) and shielded metal arc welding (SMAW) with Ni-based filler materials. Metallographic analysis revealed an unmixed region on the 304L side and a fully austenitic microstructure with carbide phases in the weld metal. Tensile testing indicated failure in the weld metal at room temperature and in the 304L base metal at 600°C, with the weld metal showing reduced impact toughness [10]. The study explored SMAW welding on API 5L Grade B PSL 2 pipes, utilizing different repair welding techniques. Macro- and microstructural analysis revealed a uniform macrostructure, but the microstructure varied, displaying ferrite and pearlite phases. The hardness distribution adhered to API 1104 standards, with repair welding 7R showing elevated hardness. Tensile strength also met API 5L specifications, with repair welding 5R demonstrating the highest strength [11]. The study examined the effects of shielded metal arc welding on nodular cast iron using Eni-CL electrodes, focusing on microstructure, hardness, and tensile strength. Metallographic analysis showed phase changes, with the heat-affected zone displaying the highest hardness. Post-welding tensile strength was reduced, highlighting the impact of welding on the material's properties [12]. An experimental study explored the relationship between welding parameters—such as electrode distance, welding speed, and gas flow rate—and weld bead geometry, while keeping torch voltage and welding current constant. Taguchi methods were used to conduct 12 experiments on 400x200x16mm samples to optimize the process parameters. The optimal settings were found to be a welding speed of 40 cm/min, a gas flow rate of 18 l/min, and an electrode distance of 45 mm, which produced the best results [13]. An experimental study on Gas Tungsten Arc Welding (GTAW) of AISI 304 and AISI 201 stainless steels optimized welding conditions. The parameters investigated included a welding current of 75 amps, pure argon with up to 8% nitrogen, and a welding speed ranging from 2 to 3.5 mm/s. The optimal results were achieved with 1% nitrogen mixed in argon and a welding speed of 3 mm/s, which enhanced weldability and corrosion resistance [14]. The optimization of Ti 6Al 4V shape welded joints was carried out using the Taguchi method with an L9 orthogonal array. The TIG welding parameters, including voltage, travel speed, and current, was varied. ANOVA, signal-to-noise (S/N) ratio, and GMEP analysis were used to determine the optimal settings, which were found to be a welding voltage of 18V, a travel speed of 70 mm/min, and a welding current of 120A [15]. The mechanical properties of Inconel 625 were evaluated using Plasma-Coupled Gas Tungsten Arc Welding (PCGTAW) on a 120x50x5mm V-groove specimen with ERNiCrMo-3 filler material. Hardness testing, tensile testing, and SEM-EDAX analysis were conducted to assess the material's performance[16]. This study focused on developing a standard welding procedure for C45 (AISI 1045) alloy to enhance its weldability through preheating and post-weld heat treatment (PWHT). SMAW and GMAW welding processes were utilized, with electrode selection following ASW standards A5.1 and A5.5. Welding samples were prepared in accordance with ASME pressure vessel codes. A comparison of E7018, E9018, and ER70S-6 electrodes was conducted based on tensile, bending, and dye penetration tests to identify the most suitable option for defect-free welding. The research resulted in a standard operating procedure for welding 16mm thick C45 plates, applicable

across various industries [17]. The MS specimen was used to assess the Degree of Penetration (DoP), hardness, and microstructure, with welding parameters such as voltage, speed, and current as input factors. Microstructural analysis revealed differences in grain boundaries for each parameter setting, highlighting the impact of these welding inputs on the material's structure. This investigation provided insights into how variations in welding parameters affect the final properties of the welded specimen [18]. GMAW was used to weld an MS plate with copper-coated MS wire, focusing on optimizing process parameters through Response Surface Methodology (RSM). Several input parameters were considered to achieve the desired weld bead geometry. A mathematical model was developed to predict the results, and the predictions were compared with experimental values to validate the model's accuracy. This approach allowed for a more precise understanding of the relationship between the welding parameters and the resulting weld quality[19]. A 6mm thick carbon steel plate was welded in a 3F fillet configuration using GMAW to predict the optimal process parameters. The input factors included welding current, speed, and voltage, while the output factor concentrated on determining the weld bead geometry [20]. SS316L specimens were welded using GMAW, with a PCA Taguchi-based method applied to optimize the process constraints. The input parameters considered included welding current, nozzle-to-plate distance (NPD), and gas flow rate (GFR). The output responses were focused on measuring ultimate tensile strength (UTS), yield strength (YS), and percentage elongation (PE)[21]. GMA welding was performed on SS409 plates using Principal Component Analysis (PCA) combined with the Taguchi L9 array design of experiments (DOE). The input parameters included nozzle-to-plate distance (NPD), welding current, and gas flow rate (GFR). The output parameters measured were ultimate tensile strength (UTS), yield strength (YS), and percentage elongation (PE) [22]. SMA welding was used to weld high nitrogen stainless steel to study its microstructure and resistance to pitting corrosion. The research found that using chromium-nickel-based electrodes led to defect-free welds, ensuring the best possible results[23]. Welding is a crucial manufacturing process used to join metals of different shapes and sizes, whether similar or dissimilar. A recent study focused on AISI 1020 steel plates to examine the depth of penetration using Response Surface Methodology (RSM). The input parameters analyzed included electrode polarity, welding current, and torch angle, all within the framework of Shielded Metal Arc (SMA) welding [24]. The study on pearlite ductile cast iron (DCI) focused on evaluating its mechanical properties and conducting non-destructive testing using five different electrode types, along with preheating. The best results were achieved with a preheating temperature of 300°C. In addition, stainless steel plates were welded using SMAW to optimize the depth of penetration, with input parameters such as welding current, torch angle, and polarity being carefully controlled [25]. The study on welding ductile cast iron (DCI) examined its mechanical properties while varying the preheat temperature between 200°C and 400°C. It is important to avoid preheating within the 200°C to 300°C range, as this can lead to martensite formation in the Heat Affected Zone (HAZ) and a reduction in fusion size, which negatively impacts the mechanical properties. To achieve the optimal results, careful control of the preheat temperature is essential [26]. Ductile iron (DI) welding was performed using Shielded Metal Arc Welding (SMAW) and Oxy Acetylene Welding (OAW) with two different types of electrodes. Preheating led to improved results when Ni electrodes were used, as it reduced carbide formation and enhanced the ductility of the welded joints [27]. Gas Metal Arc Welding (GMAW) was used to weld Stainless Steel Grade SS304, with the aim of investigating the effects of varying heat inputs (low, medium, and high). These variations were achieved by adjusting the welding current, voltage, and speed. The results showed that low heat input produced the best outcomes in terms of tensile strength, hardness, and microstructure[28]. The study examines the welding of dissimilar metals, AISI 409 Ferritic and AISI 316L Austenitic stainless steel, using MIG welding. Specimens measuring 60x100x3mm were joined using a butt joint configuration. The Taguchi L9 array method was employed with welding current (WC) at 100, 112, and 124A, gas flow rate (GFR) at 10, 15, and 20 lpm, and nozzle-to-plate distance (NPD) at 9, 12, and 15mm. The optimal welding parameters were found to be WC at 112A, NPD at 15mm, and GFR at 15 l/min [29]. The study investigates the weldability of Grey Cast Iron (GCI) using fluxless SMAW with ENi-CI electrodes. Specimens measuring 100x100x20mm with a single V groove were welded using a heat input of 2.7KJ/mm, a travel speed of 2.5mm/s, and a current of 450A. Preheating was used to control the cooling rate of the heat-affected zone (HAZ), influencing hardness and crack formation. Higher preheating temperatures resulted in a softer weld and HAZ, while reducing hardness. Additionally, a lower weld carbon equivalent helped decrease hardness and preheating costs[30]. The study examines the welding of Ferritic ductile cast iron using SMAW with E7018 and ENi-CI electrodes. Eight 150x75x20mm samples with V-grooves were tested under different conditions. The E7018 electrode required preheating at 320°C for 2 hours, while the ENi-CI electrode did not. Preheating was found to be the most significant factor, with buttering considered the most effective technique. The results were analyzed using optical microscopy (OM), scanning electron microscopy (SEM), tensile, impact, and hardness tests[31]. The study investigates the impact of corrosion on grey cast iron surface repair for pump applications using SMAW welding with three types of electrodes: carbon steel (E7018), hardening (EN14700), and nickel-based (ENi-CI). Tests conducted included abrasion pin-on-disk and corrosion testing in a 3.5% Na-Cl solution. The results showed that nickel-based electrodes provided the best performance due to the absence or excess of phases like carbide and martensite, which positively affected the material's durability and resistance to corrosion [32]. A study investigates

the parametric optimization of Ductile Cast Iron (DCI) 500/7 Grade using the L9 Orthogonal Array (OA) Design of Experiments (DoE) with the Taguchi Grey Relational Analysis (GRA) technique. The welding process employed was SMAW (Shielded Metal Arc Welding), utilizing two different electrodes, A-540 and B-850, for joining the plates. Experiments were conducted with three input parameters—current, preheat temperature, and interpass temperature—each at three different levels, resulting in the production of 18 welded plates. These plates underwent both destructive testing (DT) and non-destructive testing (NDT). The study identifies optimal process parameters that minimize costs and time while delivering superior mechanical properties in welding.

MATERIAL & METHOD:

The experimental study, the Shielded Metal Arc Welding (SMAW) process was applied to Ductile Cast Iron (DCI) 500/7 Grade material with dimensions of 150 mm × 150 mm × 12 mm (L × B × T). The plates were cast and prepared with the chemical composition detailed below. These DCI plates were manufactured by Trufirm Pvt. Ltd., Nagpur, in accordance with the chemical and mechanical specifications of DCI 500/7 Grade, adhering to ASTM, AWS, and other relevant material standards. The SMAW process was carried out using a Diffusion DW 500 MAG Welding Machine, which operates on a three-phase supply and offers a current range of 54 to 525 Amperes. The groove angle was set at 30° on each side, creating an included groove angle of 60° between the plates, with a root gap of 1.25 mm. The final welded plates measured 300 mm × 300 mm × 12 mm (L × B × T).An L9 Orthogonal Array (OA) was used to design the experiments, considering three input parameters at three levels. A total of 18 plates were welded—9 plates using A-540 electrodes and 9 using B-850 electrodes. These plates were subjected to both destructive and non-destructive testing. The chemical composition and other specifications are provided below, and the Table 1 expresses the chemical composition of (Base Metal) BM, A-540 electrode and B-850 Electrode.

Name	C	Si	Mn	P	S	Cr	Fe	Mo	V	Cu	W	Co	Nb	Al	Ti	Zr	Sn	B	Pb	Mg	Ta	N	Ni
BM	3.652	2.414	0.461	0.057	0.013	<0.030	92.819	---	---	0.413	---	---	---	---	--	---	---	---	---	0.050	---	---	<0.020
540	1.36	1.18	0.3	0.00753	0.00635	<0.0002	40.16	0.00555	0.00023	3.55	0.00176	0.0126	0.00611	0.0533	0.0897	*****	*****	<0.0001	<0.0002	*****	*****	0.0106	53.3
850	1.24	1.03	0.113	0.00356	0.00109	0.00389	0.815	<0.0007	0.0143	0.00707	0.0208	0.00082	<0.0010	0.00772	0.15	<0.0001	0.0104	0.00075	*****	0.00724	0.0893	*****	96.5

Table 01 :- Chemical Composition of Base Metal , (BM) , 540 and 850 Electrodes

3 Designs of Experiments and Experimentations

The Taguchi L9 Orthogonal Array (OA) was employed for the Design of Experiments (DoE) to optimize the input parameters, which included Current, Preheat Temperature, and Interpass Temperature. The corresponding output parameters—Tensile Strength, Hardness, and Impact—were evaluated numerically for the weld zone. Figure presents the input parameter levels: Current (100, 110, 120 Amperes), Preheat Temperature (250°C, 300°C, 350°C), and Interpass Temperature (100°C, 200°C, 300°C). It also provides a summary of the input parameter ranges used with the welding machine. Two types of electrodes were selected for the experiments, namely the A-540 and B-850 electrodes. Before use, the electrodes were baked for 15 minutes at 100°C to ensure proper conditions. The welding current was set manually on the machine, while burners were used to maintain the required Preheat and Interpass Temperatures. A thermal gun was utilized to measure the plate temperature during preheating, welding, and Interpass stages. A specially designed fixture was employed in the welding setup to prevent deformation during the process. The root gap was initially adjusted, followed by root-run welding. Subsequent passes (Run 1 and Run 2) were completed using either straight welding or weaving techniques while maintaining the designated input parameters. A total of 18 plates were welded, with 9 plates fabricated using A-540 electrodes and 9 plates with B-850 electrodes. Table 2 provides the Current, Preheat Temperature, and Interpass Temperature values used for the L9 array in the DoE.

A	B	C
Current (Amp)	Preheat Temp (°C)	Interpass Temp (°C)
100	250	100

100	300	200
100	350	300
110	250	200
110	300	300
110	350	100
120	250	300
120	300	100
120	350	200

Table 2 :- Design of Experiments (DoE) for experimentation as L9 Orthogonal Arrays (OA)

Figure 01:- 9 Welded Plate with A-540 Electrode & B- 850 Electrodes

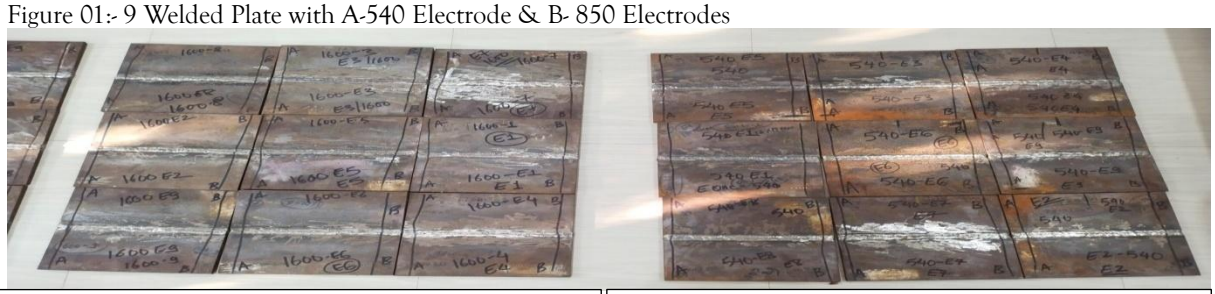

B 1 to B 9 Welded Plate with 850 Electrode | **A 1 to A 9 Welded Plate with 540 Electrode**

Figure 1 expresses the final welded plate with A-540 Electrode and B-850 Electrode (9 Welded plate by A-540 electrode and 9 Welded plate by B-850 electrode i.e total 18 final welded plates by using L9 OA).

4. Testing of Welded plate

The different types of (Destructive Testing) DT like tensile testing, hardness testing, and impact testing were performed on the 18 welded plates to achieve the numerical values as an output parameter. Apart from this different types of (Non Destructive Testing) NDT were performed like (Magnetic Particle Inspection) MPI, (Dye Penetration Test) DPT, (Radiography Testing) RT, and visual inspections were performed. The 18 welded plate of 300*300*12 mm were cut in different size as per the ASME & ASTM standards for DT & ND testing. The plates were cut in different dimensions to achieve the numerical value i.e output response like (Tensile testing, Hardness testing, Impact testing) of welded zone (WZ) and for ND Testing. The table shows the name of testing, their relevant dimensions in term of (L*B*T) form with their particular images. The tensile testing was performed on (Universal Testing Machine) UTM, hardness testing was performed on Hardness tester and Impact testing was performed on the Charpy testing machine. The figure 2 specifies the sample welded plate cut into different sections of DT & NDT sample as per the ASME Section.

Figure 02 :- Sample Welded plate with before cutting and after cutting

5. Optimization and testing results.

To find the optimum parametric conditions for all the welding process i.e SMAW (Shielded Metal Arc Welding Process), multi-objective optimization performed and for the same 'Grey Relational Analysis' was used. For the current investigation, the "smaller the better" objective function was selected for hardness, impact and tensile.

Sr.N	Exp No	Process Parameters			Output Response			Grey Relational Coefficient of output response			GRG	Rank
		Current (Amp)	Preheat Temp (0C)	Interpass Temp (0C)	HWZ (BHN)	IWZ (J)	UTS (MPA)	HWZ	IWZ	UTS		
1.	1A	100	250	100	48.67	8	358.53	0.478	0.500	0.660	0.546	5
2.	2A	100	300	200	48	8	225.72	0.579	0.500	0.333	0.471	8
3.	3A	100	350	300	48.67	8	346.49	0.478	0.500	0.605	0.528	6
4.	4A	110	250	200	48.34	10	382.84	0.524	0.333	0.803	0.553	4
5.	5A	110	300	300	50.34	8	362.57	0.333	0.500	0.679	0.504	7
6.	6A	110	350	100	48.34	8	404.95	0.524	0.500	1.000	0.675	2
7.	7A	120	250	300	46.67	6	379.08	1.000	1.000	0.776	0.925	1
8.	8A	120	300	100	48.34	8	381.82	0.524	0.500	0.795	0.606	3
9.	9A	120	350	200	49	10	333.88	0.440	0.333	0.558	0.444	9
10.	1B	100	250	100	48	6	312.38	0.455	1.000	0.381	0.612	3
11.	2B	100	300	200	46.33	6	352.81	0.653	1.000	1.000	0.884	1
12.	3B	100	350	300	48	12	340.03	0.455	0.333	0.661	0.483	6
13.	4B	110	250	200	49.33	10	334.29	0.366	0.427	0.573	0.455	7
14.	5B	110	300	300	48	10	350.61	0.455	0.427	0.919	0.600	4
15.	6B	110	350	100	50	10	316.17	0.333	0.427	0.404	0.388	8
16.	7B	120	250	300	45	8	303.1	1.000	0.602	0.333	0.645	2
17.	8B	120	300	100	48	10	336.47	0.455	0.427	0.604	0.495	5
18.	9B	120	350	200	50	10	313.29	0.333	0.427	0.386	0.382	9

Table 3:- Process Parameters values with respect to their output responses, normalised value, GRG and Rank

The table 3 the Process Parameters (Input Parameters viz current, preheat and interpass temperature) values with respect to their output responses i.e the DT (Destructive Testing) like (Hardness in BHN, Impact in Joule and Ultimate Tensile Strength in MPa), their normalized value, GRG and Rank.

Sr.No	Plate No.	Current (Amp)	Preheat Temp (^{0}C)	Interpass Temp (^{0}C)	DPT		MPT		RT	Visual	Remarks
					Front Plate	Back Plate	Front Plate	Back Plate	Seg AB	Front & Back	
1	1A	100	250	100	NSD	NSD	NSD	NSD	Porosity	NSD	Accepted
2	2A	100	300	200	NSD	NSD	NSD	NSD	Porosity	NSD	Accepted
3	3A	100	350	300	NSD	Porosity	NSD	NSD	Porosity	NSD	Accepted
4	4A	110	250	200	NSD	NSD	NSD	NSD	NSD	NSD	Accepted
5	5A	110	300	300	NSD	NSD	NSD	NSD	Porosity	NSD	Accepted
6	6A	110	350	100	NSD	NSD	NSD	NSD	Porosity	NSD	Repair
7	7A	120	250	300	NSD	NSD	NSD	NSD	Porosity	NSD	Accepted
8	8A	120	300	100	NSD	NSD	NSD	NSD	Porosity	NSD	Accepted
9	9A	120	350	200	NSD	NSD	NSD	NSD	Porosity	NSD	Accepted
10	1B	100	350	300	NSD	Porosity	NSD	NSD	Slag	NSD	Accepted
11	2B	110	250	200	NSD	NSD	NSD	NSD	***Cluster***	NSD	Accepted
12	3B	110	300	300	NSD	Undercut	NSD	Linear Indications	Porosity	NSD	Repair
13	4B	110	350	100	NSD	NSD	NSD	NSD	Porosity	NSD	Accepted
14	5B	120	250	300	NSD	NSD	NSD	NSD	Burn Thir	NSD	Accepted

15	6B	120	300	100	NSD	NSD	NSD	NSD	Porosity	NSD	Accepted
16	7B	120	350	200	NSD	NSD	NSD	NSD	Porosity	NSD	Accepted
17	8B	100	350	300	NSD	Porosity	NSD	NSD	Porosity	NSD	Accepted
18	9B	110	250	200	NSD	Porosity	NSD	NSD	Porosity	NSD	Accepted

Table 4:- Process parameter with their Testing results of DPT, MPT, RT and Visual inspection of 18 welded plates

The table 5 explains the Process parameter with their NDT (Non Destructive Testing) results of DPT, MPT, RT and Visual inspection of 18 welded plates with their final remarks for NDTs. The NSD represent the No Significant Defect found on the welded plate. Out of 18 Welded plate the 16 plate were accepted and 2 plate were need to repair for proper condition, Porosity was the most recurring defect but was tolerated under acceptance criteria in most of the cases.

Level	A	B	C
1	0.5150	0.6749	0.6089
2	0.5773	0.5271	0.4893
3	0.6585	0.5488	0.6525
Delta	0.1435	0.1478	0.1632
Rank	3	2	1

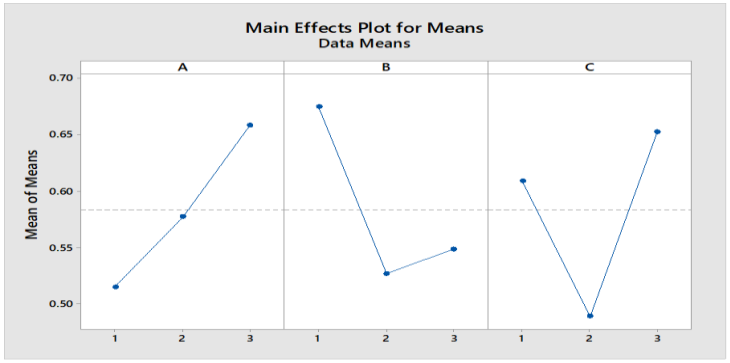

Graph 1:- Main Effect plot for means for A -540 Electrodes.

The provided Main Effects Plot for means represents the influence of three factors—Current, Preheat Temperature, and Interpass Temperature—on a welding process using A-540 electrodes. The input levels for Current are 100, 110, and 120 Amperes; for Preheat Temperature, 150°C, 250°C, and 350°C; and for Interpass Temperature, 100°C, 200°C, and 300°C. From the plot, factor A (Current) demonstrates a positive trend, where the mean response increases as the current rises, suggesting higher currents contribute positively to the evaluated output. For B (Preheat Temperature), the relationship shows a decrease at the middle level (250°C) before recovering at the highest level (350°C). This pattern implies that moderate preheat temperatures might have a less favourable effect compared to low or high extremes. C (Interpass Temperature) displays a sharp dip at the middle level (200°C) and recovers at the highest level (300°C), indicating that intermediate Interpass temperatures negatively affect the output. This analysis highlights the significant impact of these parameters on the welding process. Understanding such trends helps optimize conditions to improve outcomes, ensuring stronger welds and better mechanical performance for the given electrode and material.

Level	A	B	C
1	0.6596	0.5708	0.4984
2	0.4813	0.6599	0.5740
3	0.5076	0.4178	0.5761
Delta	0.1783	0.2422	0.0777
Rank	2	1	3

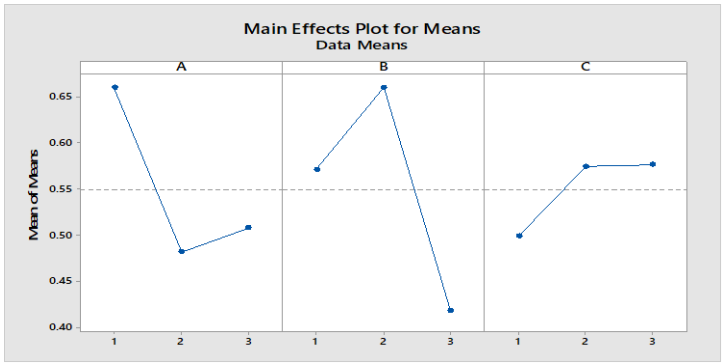

Graph 2:- Main Effect plot for means for B-850 Electrodes.

The Main Effects Plot for means illustrates the influence of Current, Preheat Temperature, and Interpass Temperature on the welding process using A-850 electrodes for nine SMAW-welded plates. The Current levels examined are 100, 110, and 120 Amperes; the Preheat Temperatures are 150°C, 250°C, and 350°C; and the Interpass Temperatures are 100°C, 200°C, and 300°C.For A (Current), the plot shows a declining trend, where the mean response decreases as the current increases. This suggests that higher current levels negatively impact the evaluated output for this specific electrode. In B (Preheat Temperature), the response peaks at the intermediate level (250°C) but drops sharply at the highest level (350°C). This indicates that moderate preheating provides the most favourable results, whereas excessive preheat reduces performance. For C (Interpass Temperature), the trend rises steadily, showing improved performance as the interpass temperature increases from 100°C to 300°C. This analysis

highlights the varying effects of input parameters on the welding process. Optimal conditions appear to depend on maintaining moderate current and preheat temperature levels while using higher interpass temperatures, ensuring better mechanical properties and weld quality with A-850 electrodes.

Table 5:- Response Values According to GRG for A- 540 Electrode					
Input Variables	***Level 1***	***Level 2***	***Level 3***	Δ	***Rank***
Current	0.515	0.5773	0.6585	0.1435	3
Preheat T	0.6749	0.5271	0.5488	0.1478	2
Interpass T	0.6089	0.4893	0.6525	0.1632	1

The table 5 show response values according to GRG for A- 540 electrode by considering the input parameters with their respective levels (1,2,3) and give the delta value for specific input variable. For A-540 electrode the highest delta value occurred at current, means current was the influential parameter of this specified outcome.

Table 6:- Response Values According to GRG for B- 850 Electrode					
Input Variables	Level 1	Level 2	Level 3	Δ	Rank
Current	0.6596	0.4813	0.5076	0.1783	2
Preheat T	0.5708	0.6599	0.4178	0.2422	1
Interpass T	0.4984	0.574	0.5761	0.0777	3

The table 6 show response values giving to GRG for B-850 electrode by considering the input factors with their particular levels (1,2,3) and give the delta value for specific input variable. For B-850 electrode the highest delta value occurred at pre heat temperature, means pre heat temperature was the significant parameter of this stated outcome.

RESULT AND DISCUSSION

This expresses the relationship between input and output parameters individually for both the electrode by using 18 welded plates.

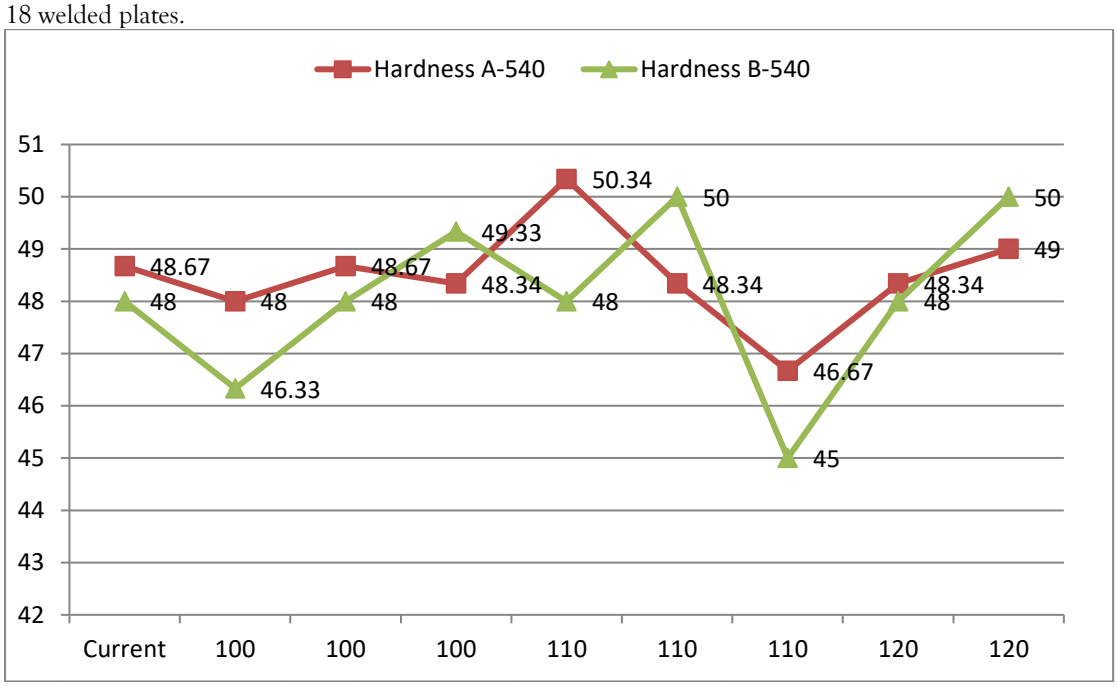

Graph 3:- Current vs Hardness of A 540 electrode & B 850 Electrodes

The graph illustrates the variation in hardness (measured in BHN) across nine experiments for A-540 and B-850 electrodes welded using the SMAW process. The X-axis represents current levels of 100, 110, and 120 amperes, while the Y-axis shows the hardness values. Electrode A-540 demonstrates relatively stable hardness values, ranging from 46.67 BHN to a peak of 50.34 BHN at 110 amperes. In contrast, electrode B-540 exhibits more significant fluctuations, with hardness dropping to a low of 45 BHN at 110 amperes and rising to a high of 50 BHN at 100 and 120 amperes. Both electrodes exhibit consistent performance at specific currents, with A-540 showing higher stability and fewer abrupt changes. This data provides insights into the mechanical properties of welded materials under different currents, aiding in optimizing electrode selection for specific applications.

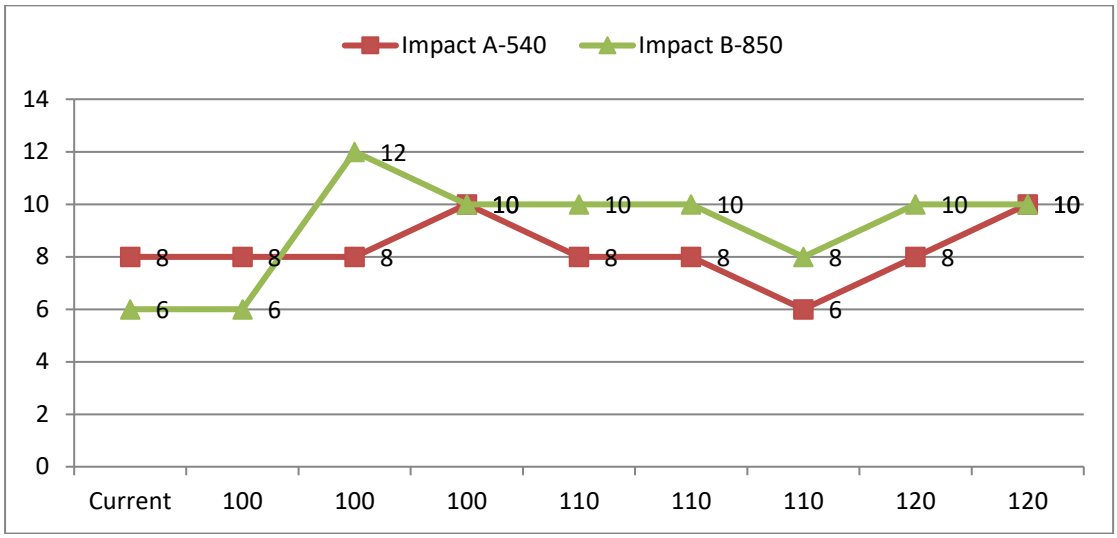

Graph 4:- Current vs Impact of A 540 & B 850 Electrodes

The graph depicts the impact energy (measured in J/m^2) for nine experiments conducted using A-540 and B-850 electrodes under SMAW welding. The X-axis represents current levels of 100, 110, and 120 amperes, while the Y-axis indicates the impact energy values. For the A-540 electrode, the impact energy remains consistent at 8 J/m^2 for most current levels, with a drop to 6 J/m^2 at 110 amperes. In contrast, the B-850 electrode exhibits a wider range of impact energy, peaking at 12 J/m^2 at 100 amperes and maintaining a stable value of 10 J/sec across 110 and 120 amperes. The results indicate that the B-850 electrode delivers higher and more consistent impact performance at higher currents compared to the A-540 electrode. This analysis highlights the difference in toughness and energy absorption between the two electrodes under varying welding conditions.

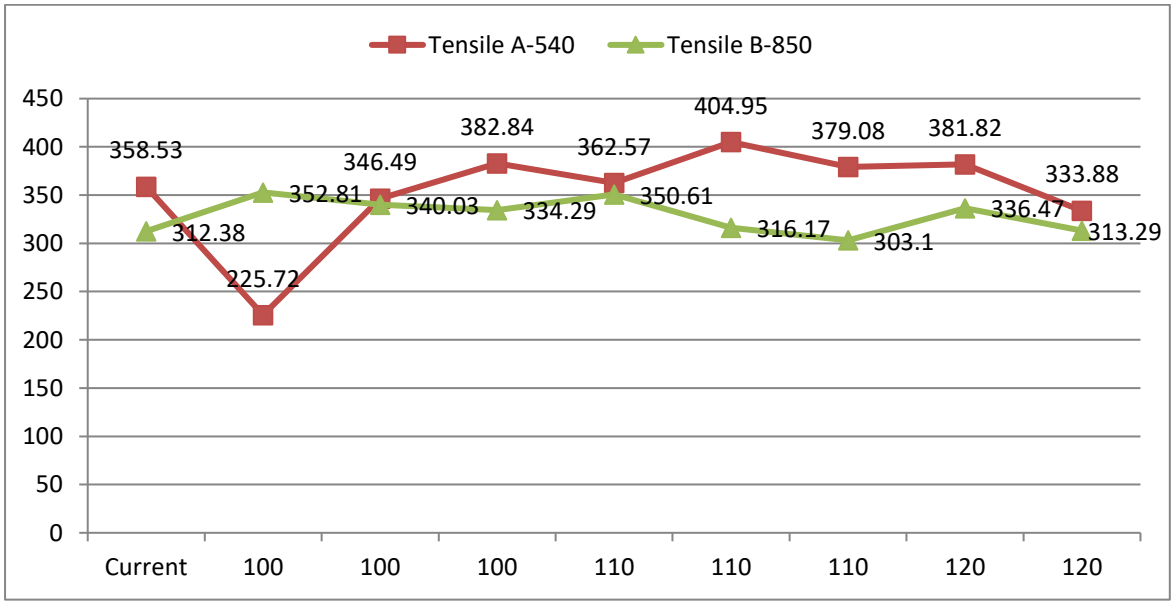

Graph 5:- Current vs Tensile Strength of A 540 & B 850 Electrodes

The graph displays tensile strength (MPa) on the Y-axis and welding current (100 A, 110 A, 120 A) on the X-axis for nine experiments using SMAW with A-540 and B-850 electrodes. The A-540 electrode shows higher tensile strength across all current levels, starting at 358.53 MPa and reaching a peak of 404.95 MPa at 110 A. For B-850, tensile strength begins at 312.38 MPa, peaks at 352.81 MPa at 100 A, and decreases to 303.1 MPa at 110 A before stabilizing near 313 MPa.Both electrodes exhibit variations in tensile strength with changes in current. The A-540 electrode generally maintains greater strength consistency, while B-850 shows more fluctuation. This suggests that the A-540 electrode is more suitable for applications demanding higher tensile strength under varying currents.

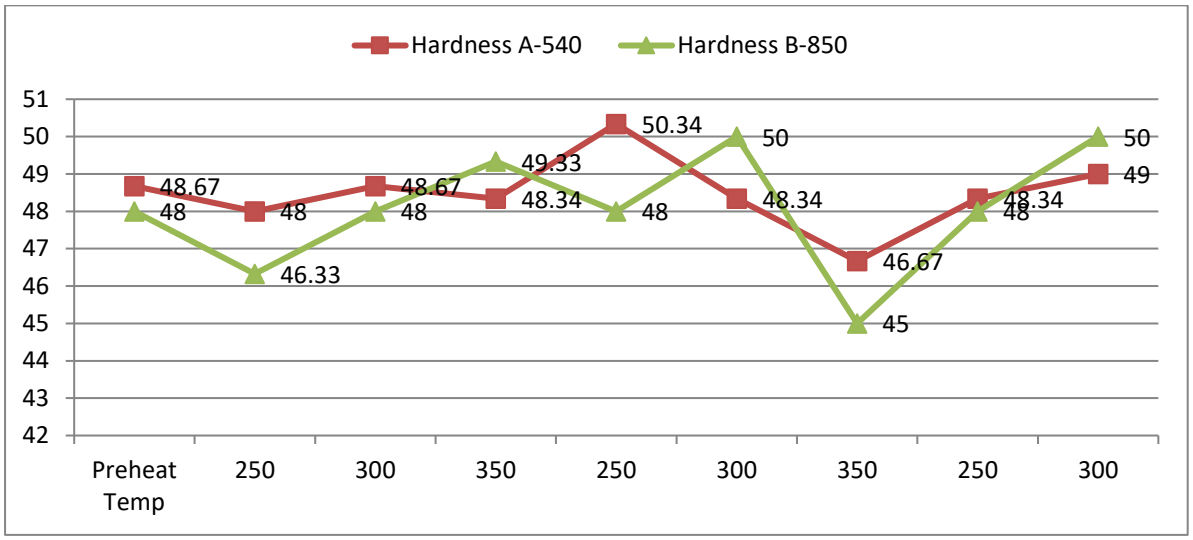

Graph 6:- Preheat Temperature vs Hardness of A -540 & B 850 Electrodes

The graph illustrates the hardness (in BHN) on the Y-axis and preheat temperature (250°C, 300°C, 350°C) on the X-axis for nine welding experiments conducted using SMAW with A-540 and B-850 electrodes. The A-540 electrode shows relatively stable hardness values, ranging between 48 and 50.34 BHN, with minor fluctuations. In contrast, the B-850 electrode exhibits greater variability, with hardness starting at 48 BHN, dropping to a minimum of 45 BHN at 250°C, and reaching a peak of 50 BHN at 300°C.Both electrodes demonstrate changes in hardness with variations in preheat temperature. A-540 maintains a more consistent performance, while B-850 shows significant fluctuations, suggesting its sensitivity to temperature changes. Overall, the A-540 electrode might be more reliable for maintaining consistent hardness under different preheat conditions, whereas B-850 offers higher hardness peaks at specific temperatures.

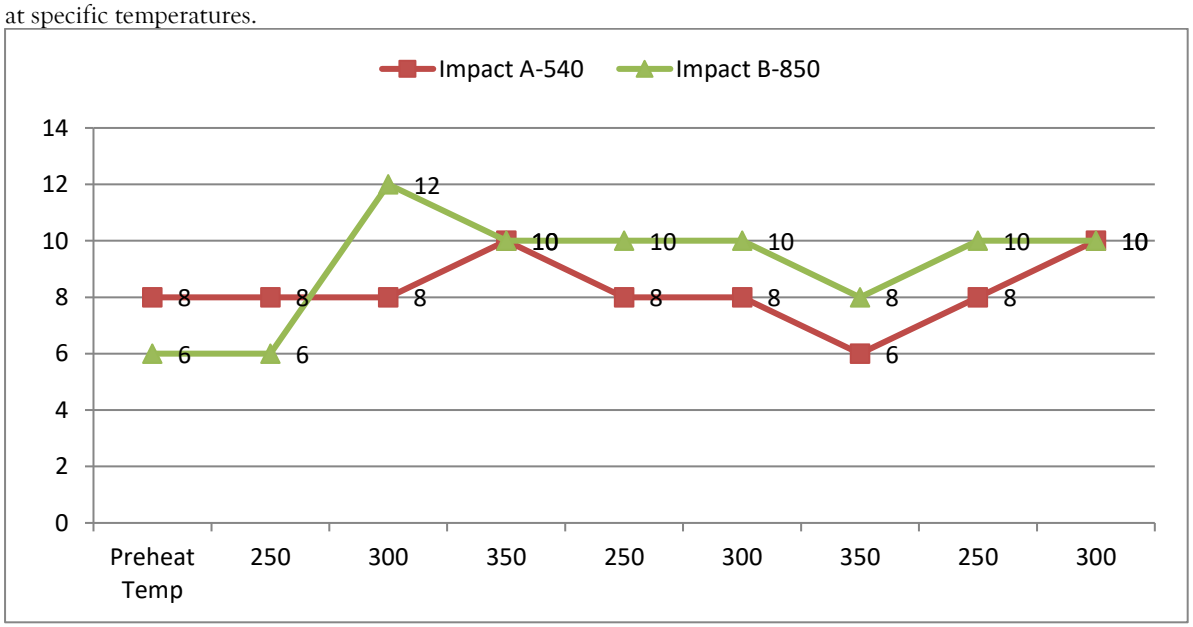

Graph 7:- Preheat Temperature vs Impact of A 540 & B 850 Electrodes

The graph depicts the impact energy (in joules) on the Y-axis and preheat temperature (250°C, 300°C, 350°C) on the X-axis for nine welding experiments using SMAW with A-540 and B-850 electrodes. The A-540 electrode demonstrates relatively consistent performance, with impact energy ranging between 6 J and 10 J. The highest value for A-540, 10 J, is observed at 300°C and 350°C, while the lowest, 6 J, occurs at 250°C.The B-850 electrode shows more variation, with impact energy starting at 6 J, peaking at 12 J at 300°C, and maintaining a steady 10 J across other temperature levels. While B-850 achieves higher impact values at specific points, A-540 maintains more consistent performance. These trends suggest that B-850 provides better energy absorption at certain conditions, while A-540 is more reliable across a broader range of preheat temperatures.

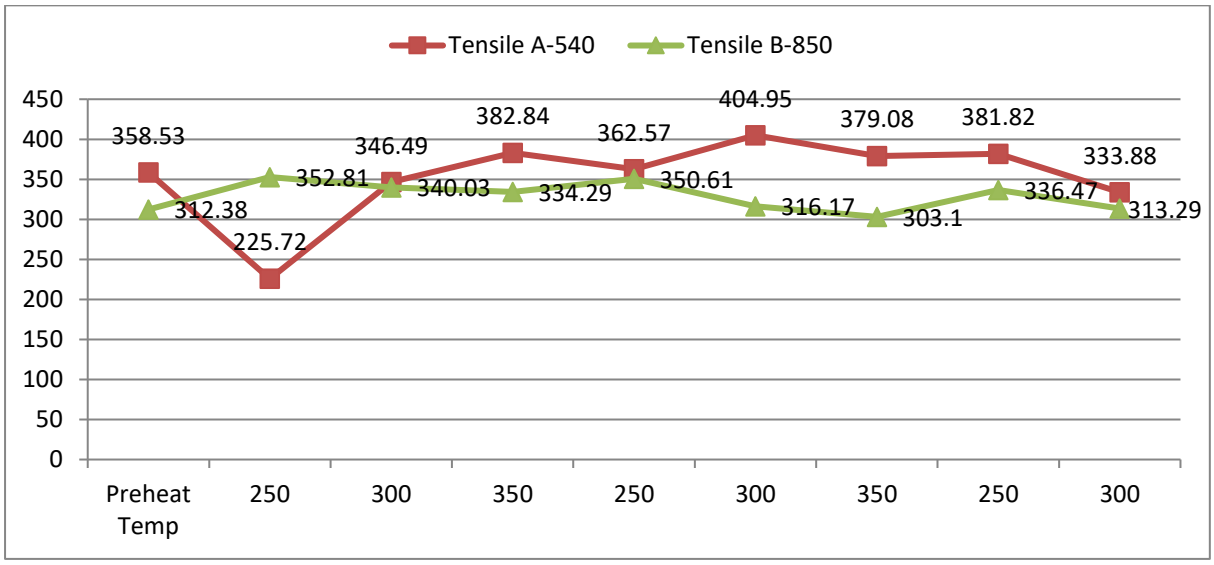

Graph 8:- Preheat Temperature vs Tensile of A 540 & B 850 Electrodes

The graph illustrates the effect of preheat temperature (250°C, 300°C, and 350°C) on the tensile strength (in MPa) for two types of electrodes, A-540 and B-850, using the SMAW (Shielded Metal Arc Welding) process. For the A-540 Electrode exhibits relatively higher tensile strength values compared to B-850 across all preheat temperatures. The tensile strength shows a peak at 350°C (404.95 MPa) and decreases slightly at 300°C (379.08 MPa) and 250°C (362.57 MPa). The B-850 Electrode tells The tensile strength values are lower compared to A-540.The peak tensile strength is observed at 350°C (352.81 MPa), with a decline at 300°C (340.03 MPa) and a significant drop at 250°C (225.72 MPa).Both electrodes exhibit improved tensile strength as the preheat temperature increases, up to a certain point. A-540 shows greater consistency and higher tensile strength performance compared to B-850. B-850's tensile strength significantly drops at the lower preheat temperature (250°C).

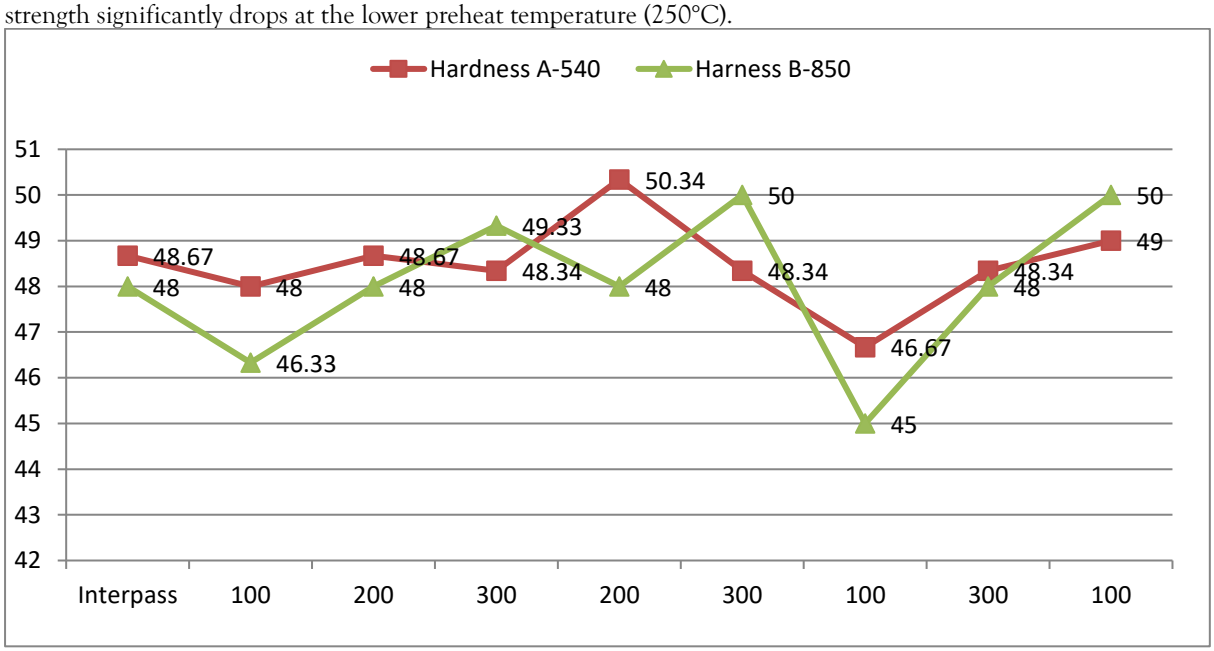

Graph 9:- Interpass Temperature vs Hardness of A 1600 & B 850 Electrodes

The graph clarifies the effect of interpass temperatures (100°C, 200°C, and 300°C) on hardness (in BHN) for electrodes A-540 and B-850 using the SMAW process. The A-540 Electrode tells the hardness remains consistent, ranging between 48 and 50 BHN, with a peak at 200°C (50.34 BHN).It shows slight fluctuations but maintains relatively steady values across all temperatures. The B-850 Electrode explain the hardness is more variable, with values ranging from 45 BHN to 50 BHN. The peak hardness is observed at 300°C (50 BHN), while the lowest value appears at 200°C (45 BHN).A-540 demonstrates better stability in hardness compared to B-850.B-850 shows significant fluctuations, with a notable dip at 200°C but recovers at 300°C.Both electrodes achieve similar maximum hardness values near 300°C.This analysis highlights the importance of temperature control for achieving consistent mechanical properties

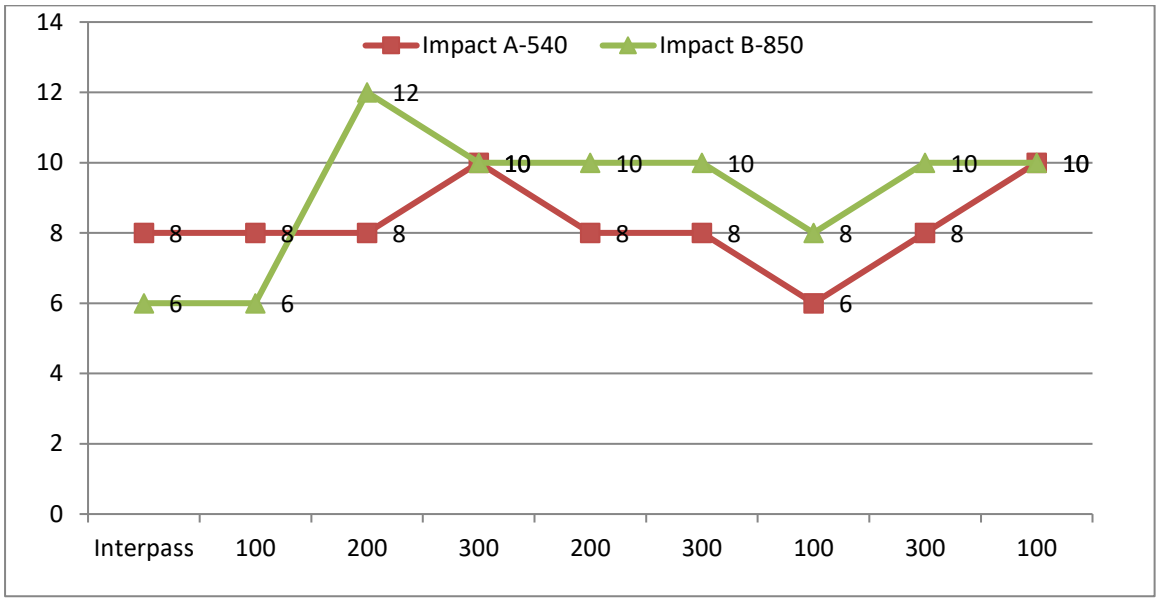

Graph 10:- Interpass Temperature vs Impact of A 540 & B 850 Electrodes

The graph compares the impact strength (in joules) of electrodes A-540 and B-850 at different interpass temperatures (100°C, 200°C, and 300°C) using the SMAW process. The A-540 Electrode has impact strength remains steady at 8 J for most conditions but decreases significantly to 6 J at 300°C.It shows consistent performance but lower overall values compared to B-850.The electrode B-850 express the impact strength is more dynamic, with a significant peak of 12 J at 200°C.It remains stable at 10 J for the majority of the other conditions, showcasing better performance compared to A-540.B-850 demonstrates superior impact strength and higher stability, except for a notable peak at 200°C.A-540 maintains consistency but with lower impact strength values.This comparison highlights B-850's better performance in impact strength, particularly at higher interpass temperatures.

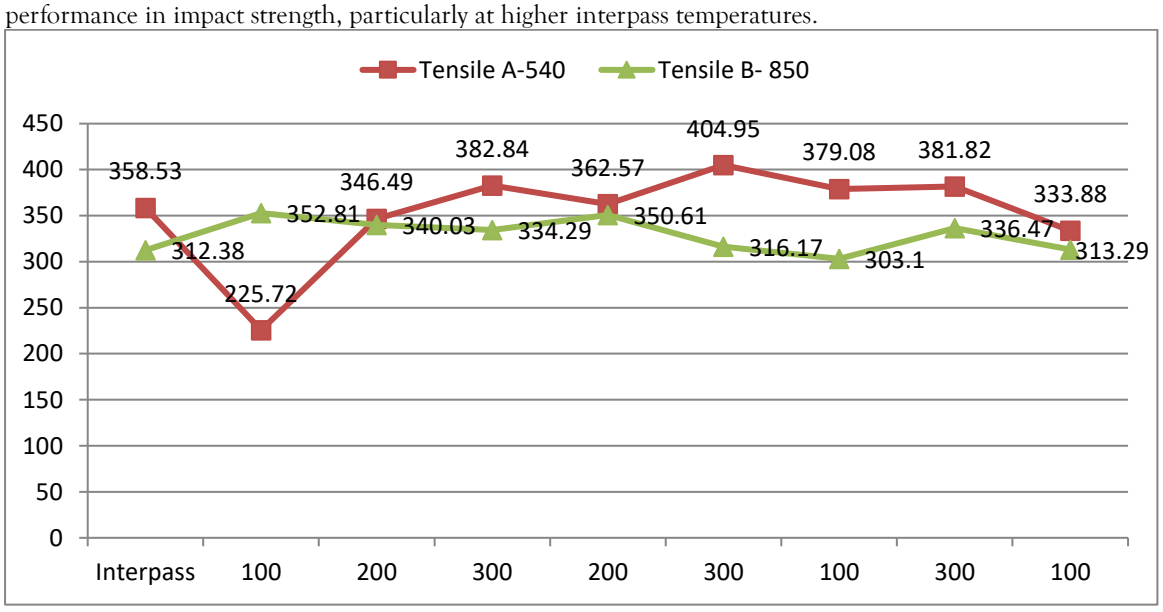

Graph 11:- Interpass Temperature vs Tensile of A 540 & B 850 Electrodes

The graph represents the relationship between Interpass Temperature (X-axis) and Tensile Strength (Y-axis) for plates welded using A-540 and B-850 electrodes. The Interpass Temperatures evaluated are 100°C, 200°C, and 300°C, while the tensile strength values correspond to nine plates welded with each electrode. For A-540 electrodes, the tensile strength shows a non-linear trend. At an interpass temperature of 100°C, the tensile strength starts relatively high at 358.53 MPa, dips significantly to 225.72 MPa at 200°C, and then recovers to its highest value of 404.95 MPa at 300°C. This indicates that lower and higher interpass temperatures favor tensile performance, while intermediate temperatures result in reduced strength. For B-850 electrodes, the tensile strength shows less variation compared to A-540. The values range from 316.17 MPa at 200°C to 352.81 MPa at 100°C, with a slight peak at 340.03 MPa at 300°C. The data suggests that B-850 electrodes maintain more consistent tensile strength across different Interpass temperatures, although their maximum values are lower than those achieved with A-540 electrodes. This comparison

highlights the significant influence of interpass temperature on tensile strength, with A-540 electrodes showing higher tensile performance but greater sensitivity to temperature changes than B-850 electrodes.

DPT (Dye Penetration Test).:-

The Dye Penetration Test (DPT), a non-destructive testing method, was conducted on 18 welded plates, nine welded using A-540 electrodes and nine using B-850 electrodes, employing the Shielded Metal Arc Welding (SMAW) process. For the A-540 plates, no surface defects (NSD) were detected in most cases, except for porosity observed on the back plate of Plate 3A (350°C preheat and 300°C interpass temperature). For the B-850 plates, NSD was common across most plates, except for specific defects: Porosity was detected on Plate 1B, 8B, and 9B under various temperature combinations. An undercut was identified on Plate 3B (300°C preheat and 300°C interpass temperature). This test highlights that both electrodes exhibit overall defect-free performance under most conditions, with occasional porosity and undercut issues. Proper temperature control and electrode selection are critical to minimizing defects during SMAW welding

.MPI (Magnetic Particle Inspection):-

The Magnetic Particle Test (MPT), a non-destructive testing method, was conducted on 18 welded plates, with nine plates welded using A-540 electrodes and nine using B-850 electrodes. The welding process utilized the Shielded Metal Arc Welding (SMAW) method, considering varying combinations of current, preheat, and interpass temperatures designed using the L9 orthogonal array (OA). For the A-540 plates, all welds showed no surface defects (NSD) across all parameter combinations, demonstrating consistent performance. For the B-850 plates, NSD was observed in most cases. However, Plate 3B (110A, 300°C preheat, 300°C interpass temperature) exhibited linear indications on the back plate. This study highlights the reliability of both electrodes under most conditions, with A-540 showing flawless results and B-850 exhibiting a single defect under specific parameters. Optimizing welding parameters is critical for achieving defect-free welds during SMAW.

RT (Radiography Test):-

Radiographic Testing (RT), a non-destructive testing method, was performed on 18 welded plates, nine using A-540 electrodes and nine using B-850 electrodes. Welding was conducted using the Shielded Metal Arc Welding (SMAW) process, with parameters such as current, preheat, and interpass temperatures designed using the L9 orthogonal array (OA). For the A-540 plates, porosity was the predominant defect, observed on all plates except Plate 4A (110A, 250°C preheat, 200°C interpass), which exhibited no surface defects (NSD). For the B-850 plates, a variety of defects were identified. Porosity was common, affecting most plates, while specific issues like slag inclusion were found in Plate 1B, cluster porosity in Plate 2B, and burn-through in Plate 5B. This study highlights that both electrodes are prone to defects under certain conditions, with A-540 demonstrating better performance and fewer defect variations compared to B-850. Proper parameter control is crucial for defect-free welds.

Visual Inspection:-

The Visual Inspection Test (a non-destructive testing method) was performed on 18 welded plates, with nine welded using A-540 electrodes and nine using B-850 electrodes. The Shielded Metal Arc Welding (SMAW) process was employed, considering current, preheat, and interpass temperatures based on the L9 orthogonal array (OA). The results revealed that all plates, regardless of the electrode type or parameter combinations, exhibited no surface defects (NSD) on both the front and back sides. This indicates that the welding parameters and techniques used were effective in producing visually flawless welds across all conditions. This outcome highlights the importance of controlled welding parameters in achieving defect-free welds when inspected visually. While visual inspection is limited to surface observations, it demonstrates that both A-540 and B-850 electrodes can consistently produce high-quality welds under the specified conditions in this study.

CONCLUSION

The study examines the relationship between input parameters—Current (in Amperes), Preheat Temperature (°C), and Interpass Temperature (°C)—and output responses—Hardness (BHN), Impact Strength (J), and Tensile Strength (MPa)—using two different electrodes (A-540 and B-850). The experiments were conducted based on an L9 orthogonal array with three levels for each input parameter. The findings are summarized below.For considering the electrode A-540, the Experiment number 7 gives the best result as per the optimization technique Gray Relational Analysis.The Experiment 7 for the electrode A was current at 120 ampere , pre heat at 250 ^{0} C and Interpass temperature at 300 ^{0} C for input factors gives the output factors as Hardness at 46.67 BHN, Impact at 6 and tensile strength at 379.08 MPa at welded zone. The Interpass temperature is the most influential input parameter for Electrode A-540.The state of Electrode B -850, the Experiment number 2 gives best optimal result as per GRA technique. The experiment number 2 states the input parameters as current at 100 ampere, preheat at 300 ^{0} C and Interpass temperature at 200 ^{0} C for output parameters as hardness at 46.33 BHN , impact at 6 and tensile strength at 352.81 MPa at welded zone. The Preheat temperature was plays the significant role as input

parameter for Electrode B-850 The other testing like visual inspection by experts, DPT (Dye Penetration Test) , MPI (Magnetic Particle Inspection) , and RT (Radiography Testing) also done for both the electrodes viz A-540 & B-850 for 18 welded plate. The confirmation test for both the electrodes A & B gives the better result.

The impact of current with reference to hardness, impact and tensile strength reveals that electrode A-540 offers greater stability in hardness and higher tensile strength across varying currents, making it suitable for applications requiring consistent mechanical properties. In contrast, B-850 shows superior impact energy, especially at higher currents, indicating better toughness. Electrode selection should depend on whether strength or impact resistance is prioritized.The influence of pre heat temperature with reference to output parameters shows that A-540 electrode maintains more consistent hardness, impact energy, and higher tensile strength across varying preheat temperatures, making it more reliable for stable mechanical performance. In contrast, B-850 demonstrates greater sensitivity to temperature changes, offering higher peak impact energy and hardness at specific points but with less consistency, especially in tensile strength.The analysis reveals that A-540 electrodes provide more stable hardness and higher peak tensile strength, but are more sensitive to interpass temperature changes, especially at 200°C. B-850 electrodes show greater impact strength and more consistent tensile performance, though with lower maximum values. Thus, A-540 suits strength-focused applications, while B-850 excels in impact resistance and stability.

REFERENCES

1. Sirohi S, Kumar N, Kumar A, et al. Metallurgical characterization and high-temperature tensile failure of Inconel 617 alloy welded by GTAW and SMAW—a comparative study. Proceedings of the Institution of Mechanical Engineers, Part L: Journal of Materials: Design and Applications. 2023;237(9):2046-2067. doi:10.1177/14644207231171266
2. Qazi, M.I.; Akhtar, R.; Abas, M.; Khalid, Q.S.; Babar, A.R.; Pruncu, C.I. An Integrated Approach of GRA Coupled with Principal Component Analysis for Multi-Optimization of Shielded Metal Arc Welding (SMAW) Process. Materials 2020, 13, 3457. https://doi.org/10.3390/ma13163457
3. Khan, M.S., Abas, M., Qayyum, Z. et al. Effect of root pass removal procedures on mechanical and microstructural properties of shielded metal arc welded joints. Int J Adv Manuf Technol (2024). https://doi.org/10.1007/s00170-024-13591-y
4. Vijayakumar, S., Arunkumar, A., Pradeep, A., Satishkumar, P., Singh, B., Rama Raju, K. S., & Sharma, V. K. (2024). Optimization of process variables for shielded metal arc welding dissimilar mild steel and medium carbon steel joints. Journal of Adhesion Science and Technology, 38(2), 185–202. https://doi.org/10.1080/01694243.2023.2227461
5. H.H. Na, I.S. Kim, B.Y. Kang, J.Y. Shim, "A experiment study for welding optimization of fillet welded structure" JAMME 45/2 , pp 178-187, 2011.
6. Rudreshi Addamani, H V Ravindra, Ugrasen G, Praveen Kumar N, Darshan C S, "Estimation and Comparison of Welding Performances using MRA and GMDH in P-GMAW for ASTM 106 Material", Materials Today Proceedings 5, pp 2985–2993, 2018.
7. I J Rohit, R. Ajithraj , M. Dev Anand, "Experimental Analysis of TIG welded 304 Stainless Steel Using Artificial Intelligence Tool",Journal of Pure and Apllied Mathematics 22 (116), pp 365-373, 2017.
8. S.Venukumar, P. Sarkar, J. Sai Sashank, P. Sampath and K Saikiran, "Microstructural and mechanical properties of Inconel 718 TIG weldments" Materials Today Proceedings 5 , pp 8480–8485, 2018.
9. Optimization of process parameters for shielded metal arc welding for ASTM A 572 grade 50 - Muhammad Saad Afzal et al Journal of Engineering Research-11 Jan 2024
10. Sirohi, S.; Pandey, S.M.; Świerczyńska, A.; Rogalski, G.; Kumar, N.; Landowski, M.; Fydrych, D.; Pandey, C. Microstructure and Mechanical Properties of Combined GTAW and SMAW Dissimilar Welded Joints between Inconel 718 and 304L Austenitic Stainless Steel. Metals 2023, 13, 14. https://doi.org/10.3390/met13010014
11. Ahmad Naufal Rizki Aini, Tara Lydwina, Asep Ridwan Setiawan Aditianto Ramelan, Assessing the Consequences of Repetitive Repair Welding in Shielded Metal Arc Welding (SMAW) on Material Properties in API 5L Grade B PSL 2 Welded Pipelines. Transactions of the Indian Institute of Metals- March 2024-04-21
12. Darmawan, A. S., Anggono, A. D., Yulianto, A., Febriantoko, B. W., Masyrukan, M., Ginta, T. L., & Hamid, A. (2024). Effect of Shielded Metal Arc Welding on Microstructure, Hardness, and Tensile Strength of Nodular Cast Iron. In 6th International Conference on Advanced Materials Science. 6th International Conference on Advanced Materials Science. Trans Tech Publications Ltd. https://doi.org/10.4028/p-2gxsxr
13. J.P. Lee M.H. Park, D.H. Kim ,B.J. Jin , J.Y. Shim , B.Y. Kang, I.S. Kim "An experimental study on optimizing for tandem gas metal arc welding process" JAMME, 68, pp 72-79, 2015.
14. Chuaiphan W, Srijaroenpramong L, "Optimization of gas tungsten arc welding parameters for the dissimilar welding between AISI 304 and AISI 201 stainless steels", Elsevier Defence Technology, pp1-6, 2018.
15. Srinivasa Reddy Vempati, K. Brahma Raju, K. Venkata Subbaiah, "Optimization of Welding Parameter of Ti 6al 4V Cruciform shape weld joint to improve weld strength Based on Taguchi Method", Materials Today Proceedings 5, pp 4948-4957, 2018.
16. Pavan Kumar Korrapati, Vaibhav Krishna Avasarala, Movva Bhushan, K. Devendranath Ramkumar*, N. Arivazhagan N, S. Narayanan, "Assessment of Mechanical properties of PCGTA weldments ofInconel 625" Procedia Engineering 75, pp 9 – 13, 2014

17. Sayed A.R., Gupta R., Barai R.,"Experimental investigation of C45 (AISI 1045) weldments using SMAW and GMAW " AIP Conference Proceedings 2148, 03004.
18. Ibrahim I. A., Mohamat S.A., Amir A., Ghalib A., "The Effect of GMAW Processes on different welding parameters" Procedia Engineering 41 (2012) 1502-1506.
19. Srivastava S., Garg R.K., "Process Parameter optimization of GMAW on IS 2062 MS using response surface methodology "Journal of Manufacturing Processes 25 (2017) 296-305.
20. Tham G., Yaakub M.Y., Abas S.K., Manurun Y.HP., Jalil B.A.,"Predicting the GMAW 3F T-Fillet Geometry and Its Welding Parameter" Procedia Engineering 41 (2012) 1794 – 1799
21. Ghosh N.,Rudrapati R., Pal P.K.,Nandi G., "Parametric Optimization of GMAW Process by PCA based Taguchi method on Austenitic Stainless Steel AISI316L"Materal Today Proceedings 5 (2018) 1620-1625.
22. Ghosh N., Pal P.K.,Nandi G., "Parametric Optimization of GMAW Process by PCA based Taguchi method on Ferritic Stainless Steel AISI409"Materal Today Proceedings 4 (2017) 9961-9966.
23. Mohammad R., Reddy M.G., Rao S.K., "Microstructure and pitting corrosion of SMAW high nitrogen Stainless Steel", Defence Technology (2015) 1-7.
24. Shukla A.A, Joshi V.S., Chel. A, Shukla B.A., "Analysis of shielded metal arc welding on depth of penetration on AISI 1020 plates using Response Surface Methodology" Procedia Manufacturing 20 (2018) 239-246.
25. E.M. El-Banna, "Effect of preheat on welding of ductile cast iron, Materials Letters 41, pp 20–26, 1999.
26. E.M. El-Banna , M.S. Nageda , M.M. Abo El-Saadat , "Study of restoration by welding of pearlitic ductile cast iron", Materials Letters 42, pp 311–320,2000.
27. M. Pascual, J. Cembrero, F. Salas, M Pascual Martinez, "Analysis of the weldability of Ductile Iron", Material Letter 62, pp 1359-1362, 2008.
28. V. Singh , M. Chandrasekaran & S. Samanta : Study on the influence of heat input on mechanical property and microstructure of weld in GMAW of AISI 201LN stainless steel, Advances in Materials and Processing Technologies, (2020).
29. N. Ghosh , Pradip Kumar Pal, Goutam Nandi, "GMAW dissimilar welding of AISI 409 ferritic stainless steel to AISI 316L austenitic stainless steel by usingAISI 308 filler wire", Elsevier ,Eng. Sci. Tech. Int. J. ,pp 1-8, 2017.
30. J.H Devletian, "Weldability of Gray Cast Iron using Fluxless Gray Iron Elctrodes for SMAW", Welding journal , pp 183-188, 1978.
31. MohsenAskari G Paykani, MehrdadShayan, MortezaShamanian, "Weldability of Ferritic Ductile Cast Iron Using Full Factorial Design of Experiment", Journal Of Iron And Steel Research, International, 2 1(2), pp 2 5 2-2 6 2014.
32. Alireza Sadeghi, Ahmad Moloodi, Masoud Golestanipour, Meysam Mahdavi Shahri, "An investigation of abrasive wear and corrosion behavior of surface repair of gray cast iron by SMAW", j m a t e r r e s t e c h n o l .6(1), pp 90–95, 2017.